The European project on high temperature measurement solutions in industry (HiTeMS) – A summary of achievements

High temperature measurement solutions in industry (HiTeMS) – a summary of achievements

G. Machin, K. Anhalt, M. Battuello, F. Bourson, A. Diril, F. Edler, C. Elliott, F. Girard, L. Kňazovická, D. Lowe, P. Pavlásek, J. Pearce, R. Strnad, M. Seifert, E.M. Vuelban

Abstract

This paper gives an overview of the achievements of the European Metrology Research Programme (EMRP) project "High Temperature Metrology for Industrial Applications" (HiTeMS). The objective of the project was to address, on a broad front, a number of unsolved measurement challenges in the domain of high temperatures above 1000 ºC, both in non-contact and contact thermometry. It brought together a total of 15 partner organisations; National Measurement Institutes (NMIs) (10), industrial companies (4) and a Fraunhofer Institute. The project started in September 2011 and was completed August 2014. Significant progress has been made in all the temperature measurement challenges tackled.

1.0: Introduction

The measurement of temperatures above 1000 ºC is vital to ensure the success of a wide range of industrial processes. However ensuring measurement reliability and, in particular, traceability to the International Temperature Scale of 1990 (ITS-90) [1] directly within the industrial process is very difficult, if not impossible in some industrial settings.

The project HiTeMS [2, 3] addressed this problem by developing a suite of methods and techniques which have the potential to significantly improved the practice of industrial high temperature non-contact and contact thermometry, up to at least 2500 °C. Special emphasis was been given to facilitating *in-situ* traceability through addressing issues such as unknown material emissivity, sensor drift and/or unquantified transmission changes.

HiTeMS was a three-year, fifteen partner project, part funded by the European Metrology Research Programme (EMRP). The project partners were: National Measurement Institutes; NPL, UK, (coordinator), Centro Español de Metrologia (CEM) Spain, CMI, Czech Republic, LNE-Cnam, France, Istituto Nazionale di Ricerca Metrologica (INRIM) Italy, PTB, Germany, Slovak Institute of Metrology (SMU) Slovakia, Turkish National Metrology Institute (UME) Turkey, VSL, Netherlands; and industrialists; GDF-Suez (GDF) France, Meggitt Sensing Systems (MSS) UK, Commissariat a l'Energie Atomique et aux Energies Alternatives (CEA) France, Endress+Hauser (E+H) Germany. In addition a Researcher of Excellence Grant (REG) was awarded to the Fraunhofer Institute for Material and Beam Technology (FhG) Germany that specializes in laser welding and materials processing. A second REG grant was awarded to the Bavarian Centre for Applied Energy Research (ZAE Bayern) after the project was started. The role of this additional partner was to perform supporting emissivity measurements of materials typically encountered in the processes covered by HiTeMs.

The research was divided into six technical workpackages each addressing a different unsolved temperature measurement problem. In brief these were:

For non-contact thermometry:

- Emissivity and reflected radiation, with the target of achieving in-situ traceability
- Self-validation and corrections for varying window/path transmission, to approximately 2500 ºC
- Real time traceable temperature measurement in laser materials processing

For contact thermometry:

- Lifetime assessment of base metal thermocouples and drift measurements of base and noble metal thermocouples
- Self-validation and demonstrated *in-situ* validation for temperature sensors to at least 2000 ºC
- Facility for determination of reliable reference functions for high temperature non-standard thermocouples

The HiTeMS project started in September 2011 and was completed in August 2014. This paper gives an overview of the main achievements of the research undertaken in the HiTeMS project. More technical details of the research can be found in the references.

2.0: Traceable and accurate measurement techniques for *in situ* surface high temperature measurement (>1000 °C)

The activities within this workpackage involved the development of various techniques for emissivity mitigated temperature measurement methods, emissivity measurement and investigation of sources of measurement uncertainty such as geometries of surfaces under measurement and large scale size-of-source effect (SSE) [4, 5].

2.1 UV-multiwavelength technique for simultaneous temperature and emissivity measurements

Multi-wavelength thermometry (MWT) is a method based on the measurement of the radiance of a source at several wavelengths. This approach is potentially attractive because from the series of multi-wavelength measurements it may be possible to determine the surface temperature and emissivity of the sample. However the method has significant pitfalls [e.g. 6] which are exacerbated through the use of the method in the visible-infrared region (e.g., 650 nm to 950 nm) leading to serious measurement accuracy issues. Current MWT systems are highly sensitive to measurement noise and model errors (errors arising from an incorrect assumption of the behaviour of the spectral emissivity). INRIM performed rigorous mathematical simulations and showed that extending the multi-wavelength method towards the ultraviolet region could lead to a significant reduction in uncertainty [REFINRIM MODEL]. The conclusion from the simulations is that by extending the operating

wavelengths down to 350 nm, the influence of both the measurement noise and model errors can be reduced considerably.

To validate the simulation, INRIM developed a prototype measurement set-up and demonstrated the feasibility of simultaneous determination of the surface temperature and emissivity. This was based on two commercially-available devices, a spectrograph Horiba Scientific model MicroHR-Auto and a TE-cooled CCD detector Horiba Syncerity 1024 x 256, coupled together. For the reference source, a commercial LAND calibration blackbody (model R1500T) was used. The MWT was fully characterized and was used in the measurement comparison using a common artefact – Inconel 600. In Table 1, the results from the temperature measurements of Inconel 600 using the MWT setup are compared with the temperature reading from a standard reference radiation thermometer (single-spot RT). Figure 1 shows the spectral emissivity of Inconel 600 measured at 900 °C as derived from the MWT. For the temperature measurement, the estimated measurement combined standard uncertainty is 5.5 °C (k=2), while for the emissivity measurement the estimated standard uncertainty is 0.072 (k=2). Further details of the MWT setup and the measurement comparison performed can be found in [7].

	t_s = 880 °C		**t_s = 900 °C**		**t_s = 920 °C**	
Measurement run	**SRT** (°C)	**MWT** (°C)	**SRT** (°C)	**MWT** (°C)	**SRT** (°C)	**MWT** (°C)
1	882.3	887.4	900.6	905.1	920.5	924
2	882.5	890.7	901	903.5	921.1	922.1
3	880.6	883.5	901.8	905.1	921.4	920
4	881.4	886.8	902.4	901.3	922.4	925
5	881.7	885.5	902.8	899.6	922.8	923
average	881.7	886.8	901.7	902.9	921.6	922.8
std.	0.8	2.7	0.9	2.4	0.9	1.9

Table 1. Temperature measurements of Inconel 600 using the MVT method.

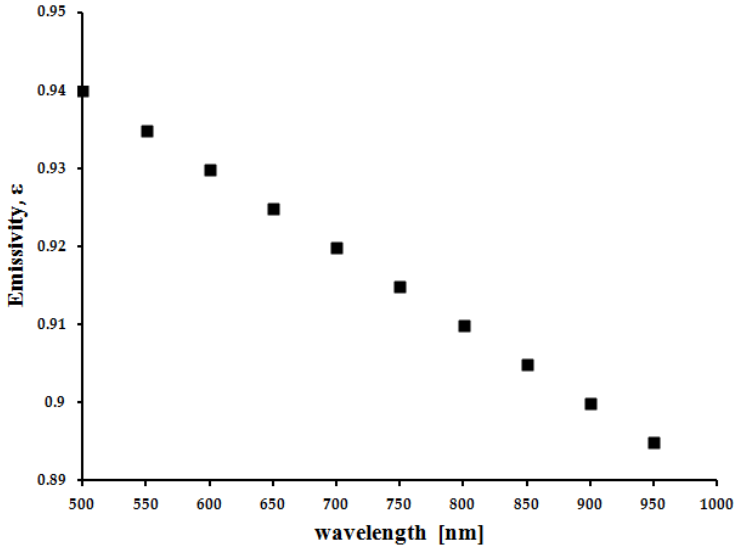

Figure 1. Spectral emissivity of Inconel 600 sample at 900 □C from the MWT measurements.

2.2 Size-of-source effect (SSE) measurements

SSE is one of the major contributors to the measurement uncertainty in radiation thermometers. For determination of the uncertainty effect of SSE in industrial settings, VSL has developed a characterization facility (Figure 2) which can simulate industrial conditions (e.g., with large background reflections, different ambient temperature conditions, varying source aperture).

Figure 2 Facility for industrial size-of-source characterization developed at VSL.

The facility has been characterized for the influence of the different aperture shapes and sizes, and the different conditions of the background radiation emanating from the wall of the furnace on the radiation thermometer signal.

Conventional methods such as direct and indirect methods for SSE determination involve the use of several sets of circular apertures with different sizes. VSL proposed a scanning method [8] for determining SSE and this was further investigated [9] with Figure 3 giving a comparison of the direct and scanning method with a fixed slit width showing the effect of variable positions from the source. More details can be found in [9].

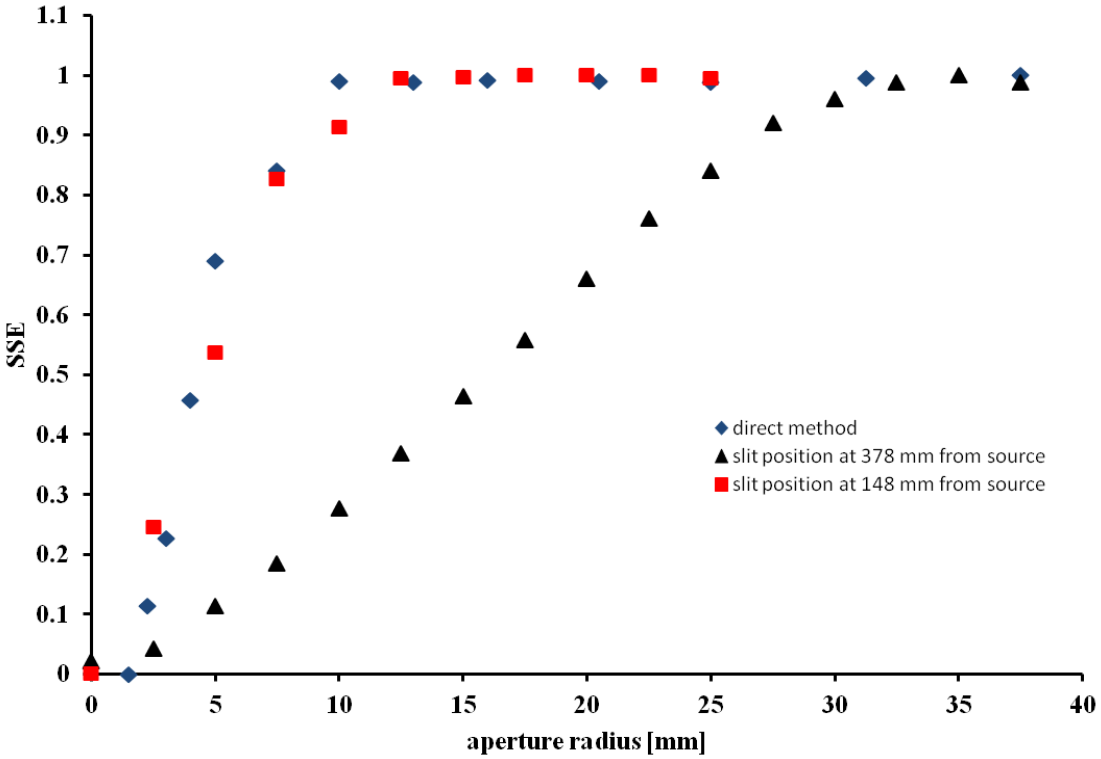

Figure 3 Comparison of the resulting SSE from: (1) direct method (blue diamond) and scanning method using a 36mm slit situated at a distance of (2) 148mm (red squares) and (3) 378mm (black triangles) from the source.

2.3 Uncertainty contribution of surface geometry on gold-cup radiation thermometers

Gold-cup radiation thermometers (Figure 4a) have been proved useful in industrial applications. These devices work by bringing a reflecting cup (often a hemisphere) close to the surface to be measured. Pseudo-blackbody radiation is established in the cup, negating the emissivity of the surface and thereby facilitating reliable temperature measurement. However, due to conditions in the field where the geometry of the surface being measured is far from ideal, the accuracy of the results provided by this type of radiation thermometer is highly influenced by the surface geometry. Typical real examples are tubular and sloping surfaces such as those commonly encountered in various processing industries. VSL has built a facility (Figure 4b+c) where cavity-based radiation thermometers can be characterized properly with different surface geometries. Characterisation results have shown that the uncertainty

associated with the measurement on a curved surface at a temperature of 700 °C could be 3.5 °C (k = 2), which accounts for more than half of the total uncertainty (6.1 °C) of the measurement. For sloping surfaces, an uncertainty contribution of the surface geometry amounts to 0.4 °C (at a maximum angle of 20°), with the overall uncertainty of 5.4 °C. These results show that metallic cup thermometry is relatively insensitive to modestly sloped surfaces but is strongly affected by curved surfaces [10].

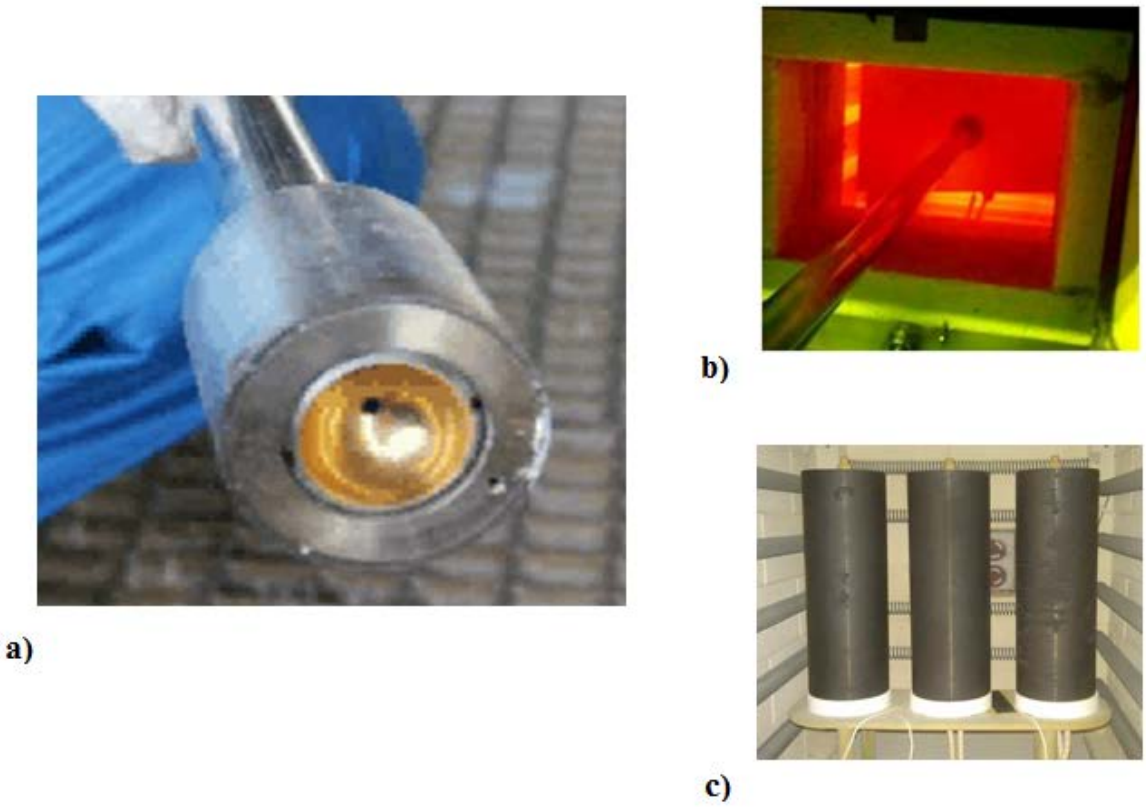

Figure 4 Characterization of a) gold-cup radiation thermometer on various surface geometries: b) sloped flat surface, c) curved surface.

2.4 Temperature-independent emissivity measurement using the virtual source technique

The virtual source method for emissivity measurement involves the creation of a so-called "virtual source" by the reflection of the source radiance onto a mirror with known reflectance. This concept is illustrated in Figure 5a. The radiant flux from the sample consists mainly of two source contributions: the thermal radiation directly coming from the source, and radiation originating from the virtual source (radiation reflected from the mirror). By changing the position of the mirror that creates the virtual source, the resulting signal changes and a typical function for each emissivity value and material is created. The next step in determination of the emissivity values is the generation of multiple functions using a mathematic model. The function creation depends on multiple variables which are present in the real measurement. By the systematic change of the values of these variables, different mathematical functions are created. Each individual function represents a different emissivity value. By using a mathematical fitting, we are able to assign the real measured curve (with an unknown emissivity) a function in which we know the emissivity. What is so attractive with

this approach is that we are able to determine precisely the emissivity without the need to perform any temperature measurement of the source. Measurements on Inconel 600 gave the same values as those found in literature hence confirming that the approach works. Further details of the model and the virtual source approach are described in [9].

3.0 WP2: Validated methodology for lifetime and drift tests for contact thermometry sensors (>1000 °C)

The objective of this WP was establish a rigorous means of determining the lifetime characteristics of base metal thermocouples and the drift characteristics of base metal and noble metal thermocouples, to high temperatures, firmly grounded in traceability to the SI (i.e. to the ITS-90).

Lifetime and drift testing capability were established at CMI (Czech Republic), LNE-CNAM (France), SMU (Slovakia) and TUBITAK (Turkey) for temperatures up to 1800 °C. Different base metal type N and K thermocouples, of varying diameter were supplied by a number of manufacturers, and in addition some noble metal R, S and B types. All the base metal thermocouples were in mineral insulated metal sheathed (MIMS) format. The outcome of the tests were not only an agreed method for sensor lifetime and drift characterisation (which has become an agreed EURAMET[1] guide) but also helped understand the basic drift characteristics and mechanisms of thermocouples.

3.1 Methodology for lifetime and drift testing of thermocouples

An outline of the procedure for lifetime and drift testing is given below, more details can be found in the EURAMET guide [11].

3.1.1 Procedure for lifetime testing of base metal thermocouples

For establishing the lifetime of thermocouples it is recommended to use new, untreated and uncalibrated thermocouples.

1. Prior to starting the test the thermocouples must not be subject to any heat treatment, e.g. calibration or annealing.
2. Use a good quality temperature standard for determining the furnace temperature (e.g. intermittent use of a noble metal type R, S or B or Pt-Pd).
3. Test the thermocouples at the desired temperature. For example, the testing temperature may be determined on the basis of the supplier's specification of the maximum allowable temperature for short term use with addition of 5 %.
4. Connect all thermocouples to the multimeter (use only a switchbox with known properties) or A-to-D converter.

[1] Euramet – European Association of National Metrology Institutes
http://www.euramet.org/index.php?id=homepage

5. Continuous measurement of the thermocouples (with automatic or manual data logging), the furnace temperature is checked with the reference thermometer periodically (e.g. once per week).
6. The test, for a given thermocouple, should be terminated if
    a. There is no output from the thermocouple, or
    b. The drift of deviation of the tested thermocouple from standard EN IEC 60584-1 exceeds the desired tolerance.

The lifetime of the thermocouple calibration is determined as the time elapsed between the start of the test (Step 3) and its termination (Step 6).

3.1.2 Procedure for drift testing

There are two aspects to the process of drift testing depending upon what the test is trying to determine, i.e. short term or long term drift, and it is anticipated that these tests will be performed at different temperatures.

Drift: short term

This test should be applied to a calibrated and properly annealed thermocouple, with the recommended procedure for determining thermocouple short term drift as follows:

1: Calibration of the test thermocouple at the maximum temperature of intended use and a homogeneity performance check [12]

2. Testing of the thermocouples at the desired temperature.

3. The duration of the test is 8 hours maximum

4. Calibration of the thermocouple at the maximum temperature of intended use.

5. Repeat steps 3 to 4 three times.

The calibration drift is determined as the change in output (or its temperature equivalent) between the first calibration and the final calibration.

Drift: long term

This test should be applied to a calibrated and properly annealed thermocouple with the recommended procedure for determining thermocouple long term drift as follows:

1: Calibration of the test thermocouple at the maximum temperature of intended use and a homogeneity performance check

2. Testing of the thermocouples at the desired temperature.

3. The duration of the test is 4 months minimum.

4. Calibration of the tested thermocouple at the maximum temperature of intended use every week during the first month and every 2 weeks for the following months.

5. The test(s) are finished if either; the agreed final time is reached, or there is no output from the thermocouple or the deviation of the tested thermocouple from standard EN IEC 60584-1 exceeds 3 times the desired tolerance.

The calibration drift is determined as the change in output (or its temperature equivalent) between the first calibration and the final calibration.

3.2 Test measurements performed with thermocouples

The procedure was tested using a range of base and noble metal thermocouples supplied by the indicated manufacturers.

	Life time	Drift long term	drift short term	drift long term	drift short term
Producer[2]	1300 °C	1000 °C a 1100 °C	1100 °C a 1300 °C	1000 °C a 1720 °C	1600 °C 1820 °C
	5 × 1 mm	3 × 1 mm	2 × 1 mm		
	5 × 3 mm	3 × 3 mm	2 × 3 mm		
Omega	5 × 6 mm	3 × 6 mm	2 × 6 mm		
	4 × 1 mm	2 × 1 mm	2 × 1 mm		
	4 × 3 mm	2 × 3 mm	2 × 3 mm		
CCPI	4 × 6 mm	2 × 6 mm	2 × 6 mm		
	4 × 1 mm	3 × 1 mm	2 × 1 mm	2 × type B	1 × type B
	4 × 3 mm	3 × 3 mm	2 × 3 mm	2 × type R	1 × type R
Meggitt	4 × 6 mm	3 × 6 mm	2 × 6 mm	2 × type S	1 × type S
	2 × 1,5 mm				
	2 × 2 mm	1 × 1,5 mm	1 × 1,5 mm		
	2 × 3 mm	1 × 3 mm	1 × 3 mm		
	2 × 4 mm	1 × 4 mm	1 × 4 mm		
Zpa Nová Paka	2 × 6 mm	1 × 6 mm	1 × 6 mm		

Table 2: Details of thermocouple suppliers and diameters, both type N and K were supplied by the manufacturers

The participating institutes, CMI (CZ), SMU (SL), LNE-Cnam (F) and UME (TU), undertook tests according to the specified procedure and sample results are given below, more results are reported in X and Y [13, 14, 15].

[2] Add details of manufacturers

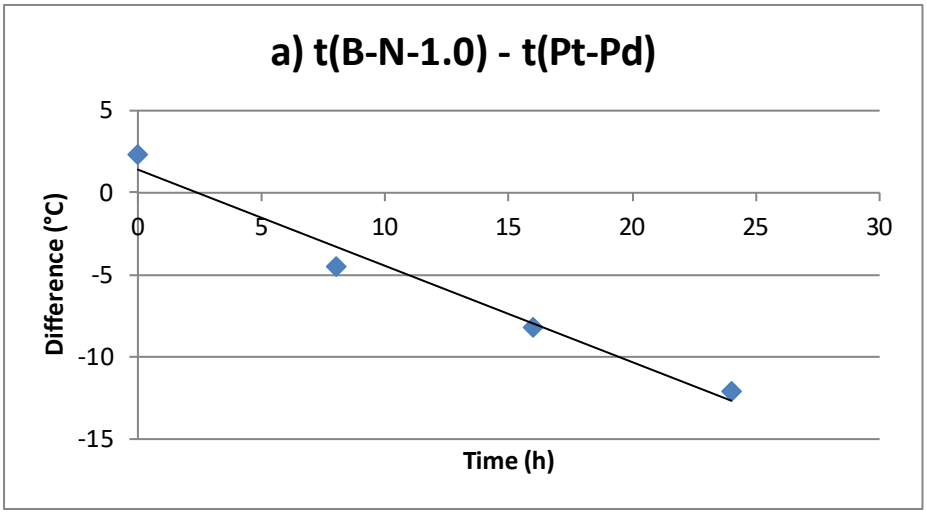

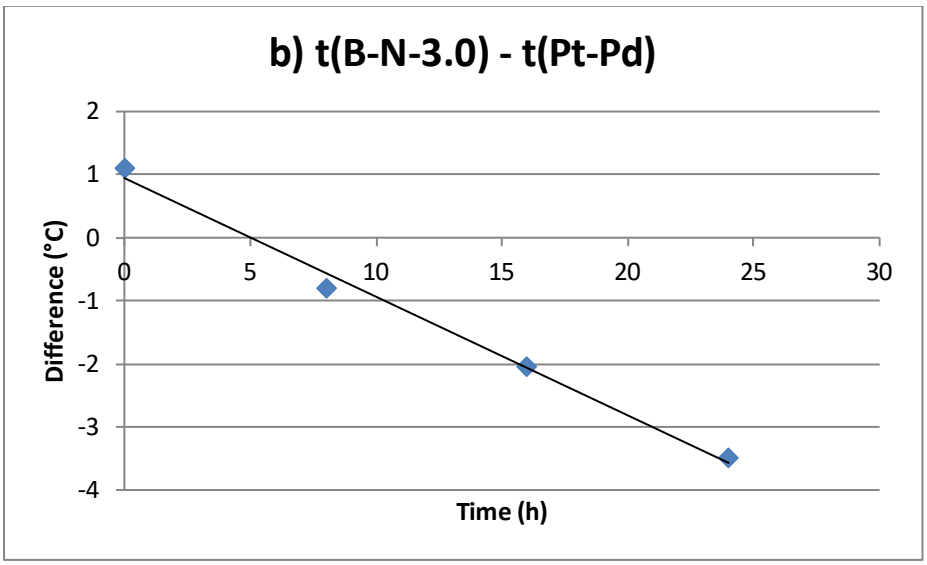

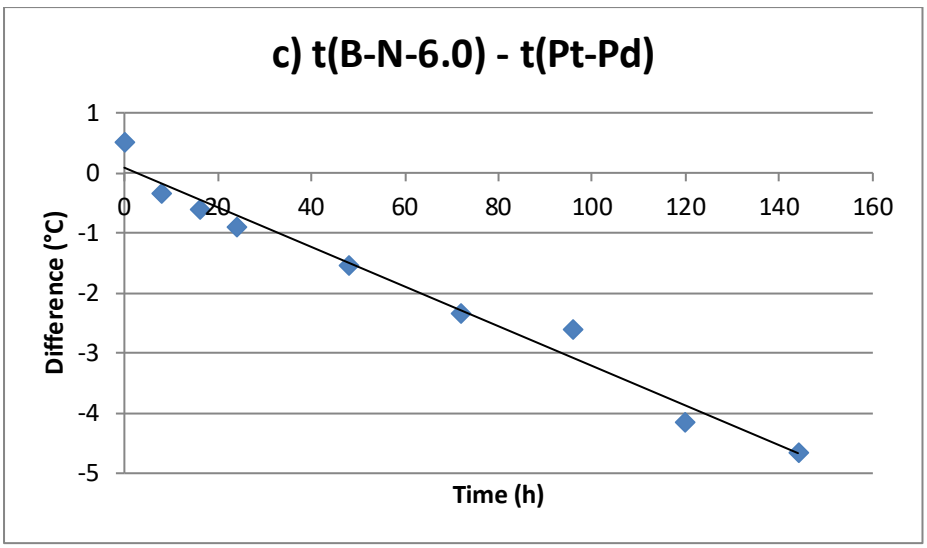

Figure 5: Typical drift measured with type N thermocouples during short-term drift tests at 1300 °C; a) 1.0 mm diameter; b) 3 mm diameter; c) 6 mm diameter

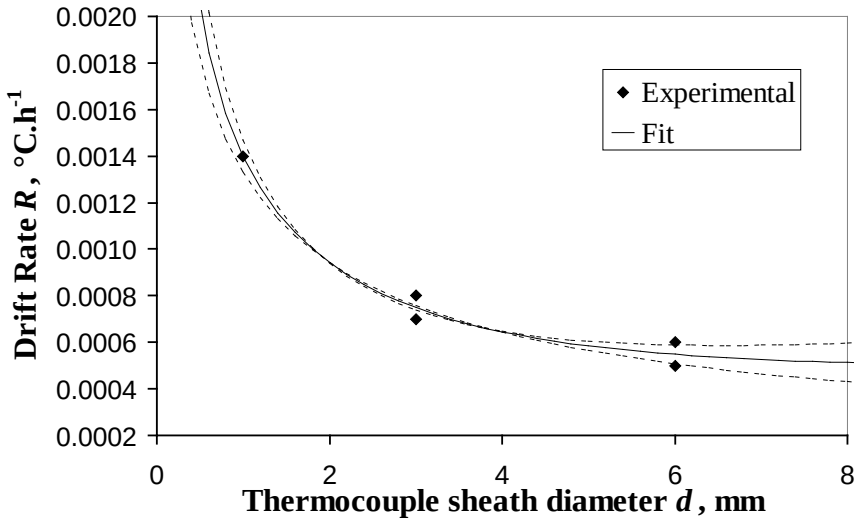

Figure 6: Influence of the diameter on the drift rate of a batch of type K thermocouples exposed to a temperature of 1000 °C during 800 h. Tolerances of the model are shown by the dashed lines.

Investigation of drift dependence with thermocouple diameter was also performed; a typical result in Figure 7 below.

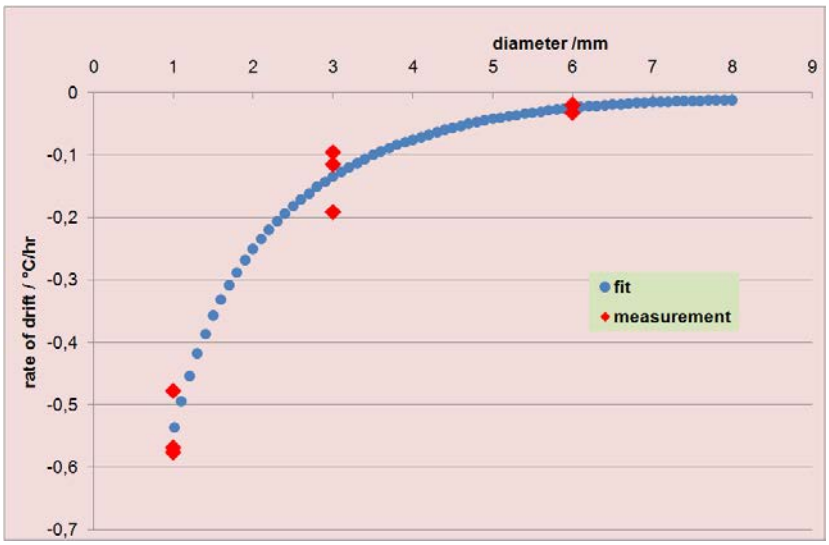

Figure 7: Rate of drift with thermocouple diameter at 960 °C (N type)

There are a significant number of thermocouple test results that cannot be included in a summary paper such as this – these can be found in [13, 14, 15].

The outcome of this work is that an agreed process for studying thermocouples drift and lifetime characteristics has been agreed across Europe and a Euramet guide developed. This has already been implemented in a number of thermocouple manufacturers facilities such as Meggitt and Zpa Nová Paka.

4.0 Self-validating contact thermometry sensors for above 2000 °C

The objective of this WP was to demonstrate mitigation of the drift of contact thermometry sensors to above 2000 ºC through self-validation. Two self-validation concepts were investigated. The first was based on the use of miniature fixed points with defined and stable melting temperatures of pure metals or metal-carbon (Me-C) eutectics, these were combined with commonly used thermocouples to detect the magnitude of the drift. The second self-validation concept is based on the simultaneous use of electrical noise thermometry as a (primary) method to measure temperatures independently of material based drift effects. A general overview about noise thermometry can be found in [16], details of the used noise thermometer are described in [17].

Material compatibility studies up to 2300 °C were performed to identify suitable materials for the use of miniature high-temperature fixed points (HTFPs) realized in mini carbon (graphite) crucibles in conjunction with tantalum or molybdenum sheathed W/Re thermocouples. This study showed that tantalum was the more suitable sheath material to high temperatures, with hafnia or yttria-stabilized zirconia suitable as insulators for the thermoelements within the tantalum sheath [18]. Two HTFPs of graphite filled with Pt-C (1738 °C) and Ru-C (1953 °C) were constructed (Figure 8). As an example of the long-term stability Figure 9 shows the measured emfs of the melts of the Pt-C cell at repeated melting and freezing cycles by using W/Re thermocouples during a heat treatment for 2225 h at $T \approx 1727$ °C. The melting temperatures of the Pt-C cell were measured before and after the heat treatment by using a radiation thermometer and agreed within 0.2 K. The measurement uncertainty of the radiation temperature was about ±1 K. The melting temperature of the Pt-C cell remains stable and the drifts observable in Figure 9 are caused by thermoelectric instabilities of the thermocouples used. Similar results were obtained by using the Ru-C cell at temperatures around 1953 °C. This clearly demonstrates the ability of the investigated miniature cells to detect drift effects of thermocouples around the order of 1 °C or less.

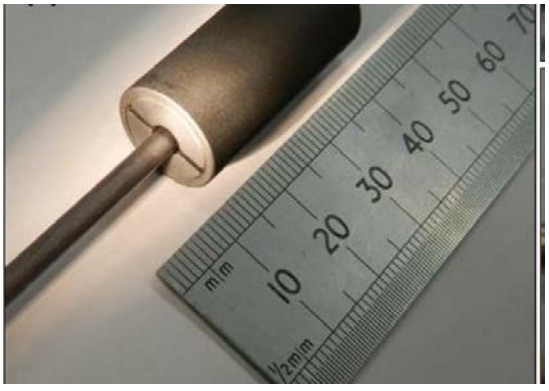

Figure 8: High-temperature miniature fixed point filled with a Me-C eutectic and usable with MIMS thermocouples

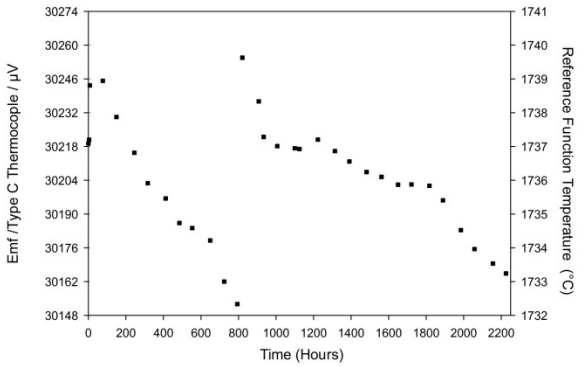

Figure 9: Emfs of the melts by using the Pt-C miniature fixed point with W/Re thermocouples

Graphite based fixed points can only be used in non-oxidising environments at these temperatures, so work was performed to develop fixed points suitable for oxidizing

environments. A number of different designs of self-validating structures usable in oxidizing atmospheres up to 1800 °C were constructed and investigated. Miniature cells were made of Alumina (Al_2O_3) 99.7% and pure metals of platinum and palladium were used as fixed-point materials. Figure 10 shows one design of the miniature fixed points [19], the fixed point material is within the alumina crucible. This was then inserted within a platinum cartridge and welded between the measurement junction of the type B thermocouple. Another self-validation method deployed the use of thick wires of pure metals in multibore insulators were used as fixed-point materials [20] this is the so-called "pulled-wire" method shown in Figure 11 (other approaches are reported in [20, 21]).

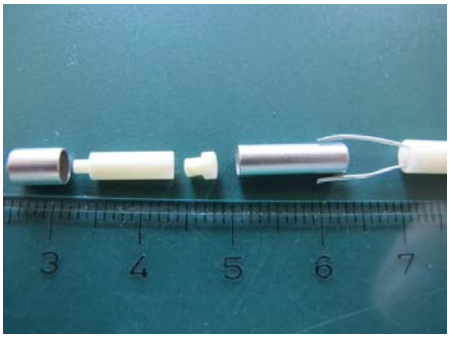

Figure 10: Miniature fixed point welded between the thermoelements

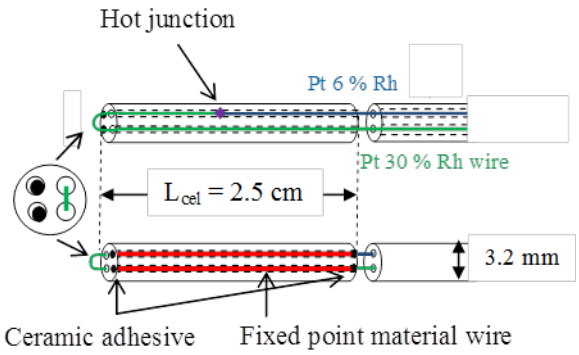

Figure 11: Integrated self-validating pulled-wire (PW) module

Typical melting curves by using type B thermocouples with the integrated self-validating fixed points or the pulled wire modules are characterized by a constant increase of the emf before the melting process starts and a decreased slope during the melting process. This is because the measurement junction is to a lesser or greater extent exposed to the furnace environment. Both parts (before the melt and during the melt) can be approximated by regression lines and the intersection point of the two straight lines corresponds to the emf of the melting point. A special feature of the melt by using this type of integrated fixed-point was the dependency of the melting temperature on the heating rate, since the measurement junction is not or only partially surrounded by the fixed-point material. Therefore, the measurement is sensitive to the heat flux from the furnace and an extrapolation of the emfs to adiabatic conditions is necessary for highest accuracy. Typical measurement uncertainties (k = 2) of the melting temperatures of the used fixed-point materials were in the order of ±1.7 K. The self-validating concept based on integrated miniature fixed-point cells and self-validating

structures usable under oxidizing conditions was found to be usable to detect drift effects of thermocouples in the order of about 2-3 K.

A final approach to drift mitigation is through the direct measurement of thermocouple drift by a completely different thermometry technique. In HiTeMS this was through using (primary) electrical noise thermometry – which is too slow to use as a practical sensor for process control - but should (in principle) be driftless over long periods of time and hence suitable for sensor drift monitoring.

To test this approach two combined thermocouple-noise temperature sensors based on noble metal thermocouples (type S and type B) and usable in oxidizing atmospheres were constructed. A detailed description of the sensors can be found in [22]. Noise temperature measurements at the freezing points of copper (1084.62 °C) and silver (961.78 °C) agree to the fixed-point temperatures within about 0.4 K and within 0.2 K, respectively. These results demonstrate the accuracy of the combined thermocouple-noise temperature sensors and of the noise thermometer electronics used within an uncertainty of at least ±1 K (k = 2). The long-term stability of one of the combined sensors was tested at 1100 °C and 1340 °C for 560 hours and 600 hours, respectively. The noise temperatures and the thermocouple temperatures were measured periodically (every 50-100 h). No drift of the two type S thermocouples of the combined sensor was detectable which indicated their excellent thermoelectric stability. The measured noise temperatures remain constant and agree very well with the thermocouple temperatures within about ±0.3 K at 1103 °C. At 1340 °C a systematic difference between the two thermocouple temperatures and the noise temperature of about 2 K was found, it remained constant during the first 250 hours but decreased slightly by about 1 K during the next 350 hours caused by a change in the value of the noise resistance. Nevertheless this apparent drift was within the relative measurement uncertainty of the noise temperature of about (0.1-0.2) % (k = 2).

The accuracy of the noise temperature measurement was also checked by a simultaneous measurement of the temperature by using a silicon photodiode based radiation pyrometer. The results of the measurements are presented in Figure 12. The error bars corresponds to the statistical uncertainty (k = 1) of the electrical noise temperatures (ENT). The good agreement of the noise temperature and the radiation temperature indicates the high accuracy of the absolute noise temperature measurement also at higher temperatures than given by the two fixed points of the ITS-90. The patterns of temperatures measured by the three independent methods show also a high conformity. The uncertainty of the radiation temperature was of order ±1.5 K (k = 2).

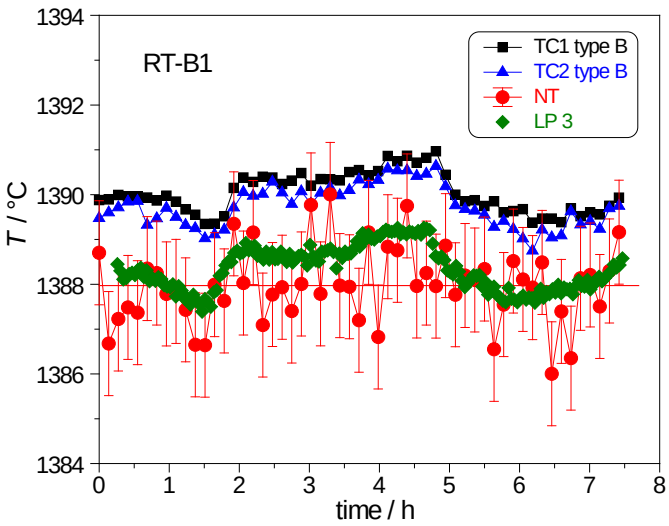

Figure 12: Check of the accuracy of the electrical noise temperature measurement by using silicon photodiode based radiation pyrometer to measure the temperature independently

5.0 Validated methods for non-contact thermometry above 2500 °C including novel self-correcting techniques

The objective of this part of the project was the implementation and testing of self-validation techniques up to 2500 °C for non-contact thermometry facilitating the correction of stochastic thermometer and/or for progressive window transmission changes. The method for determining these thermometer changes used HTFP blackbody cavities incorporated within the tested environment. The principle is quite straightforward the radiation thermometer periodically views the HTFP whose temperature is known. The apparent melting temperature is measured when viewing through the window, then from this measurement, and from knowing the temperature of the HTFP the window transmission can be deduced, and hence corrected for.

This research was split in two parts:

- The development and characterisation of robust HTFPs suitable for industrial use in inert atmospheres;
- Implementation of the HTFPs in industrial conditions and assessment of their capabilities for varying window transmission correction.

5.1 The development and characterisation of robust HTFPs suitable for industrial use

Several cells, at the fixed-points of Co-C (1324 °C), Ru-C (1954 °C) and Re-C (2474 °C) were constructed in the three NMIs, LNE-Cnam, UME and NPL, a schematic diagram of the

HTFPs can be found in Figure 13. The characteristation and testing of the cells can be found in [1, 2].

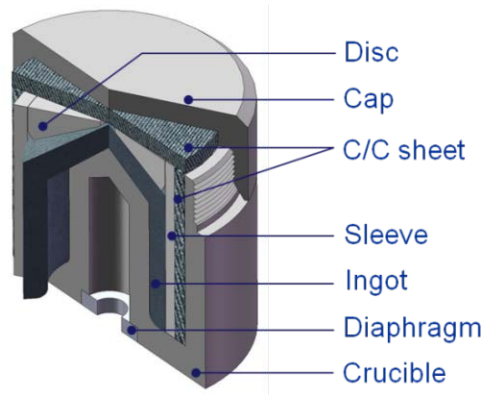

Figure 13: Schematic diagram for the graphite cell for Co-C, Ru-C and Re-C HTFP blackbody. Dimensions are 24 mm length, 24 mm diameter and cavity dimensions of 5 mm diameter and 15 mm length (emissivity of 0.996, reaching 0.999 with the 3-mm added aperture).

A typical result is shown in Fugure 14 showing a typical melt and freeze cycle of a robust Co-C cell. This Co-C cell has undergone 4 melt and freeze cycles performed in a high temperature furnace with setpoints of +/- 400 °C around the melting temperature. These set points led to very rapid heating typical of what is encountered in industry, nevertheless the cell was undamaged demonstrating robustness [23].

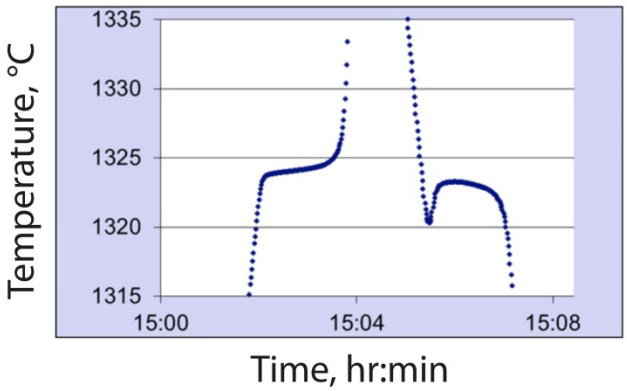

Figure 14: x-axis time, y-axis temperature in °C. Performance of a robust Co-C of design shown in Figure 7. Plateau duration ~1 minute. Melting range ~0.350 °C

5.2 Implementation of the HTFPs in industrial conditions and assessment of their capabilities for varying window transmission correction

Six of the HTFP cells were transported to CEA Cadarache (close to Marseille, France) and studied in the VITI induction furnace (Figure 15a). This furnace is part of the facilities

devoted for the study of the properties of corium in the laboratory for control of severe accidents (LPMA) [24].

The main output of these tests was that all the cells tested in the VITI furnace withstood the large heating and cooling ramps of up to 150 K/min. The plateaux could be observed using a radiation thermometer through a window allowing an *in-situ* recalibration of the furnace temperature control pyrometer. Cycling of the cells around the corresponding melting temperatures was performed. Figure 15-b shows a typical pattern of cycling of Re-C cells during which multiple plateaux were recorded with very large heating/cooling rates and overheating which could reach 400-500 °C. In all cases, the plateaux were still usable.

These measurements allowed for the testing of window transmittance correction methods. The effect of window transmission on the measured temperatures was studied and an algorithm developed to help correct for this effect by the use of *in-situ* HTFPs [25, 26].

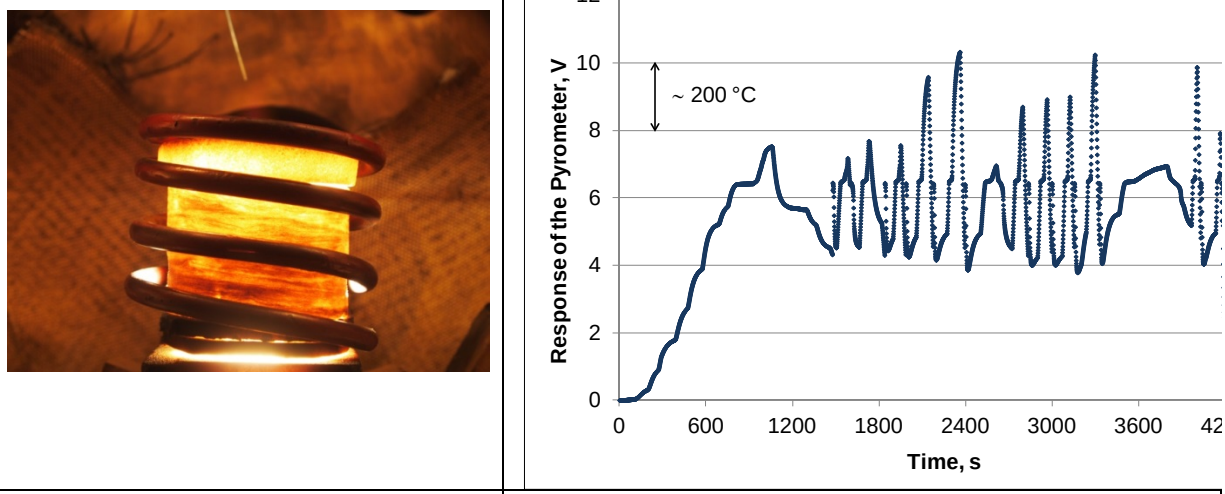

Figure 15: (a) Installation of the HTFP cells in the CEA VITI induction furnace and (b) the results of the cycling of the NPL Re-C cell.

The research performed successfully demonstrated the use of HTFP blackbody sources as suitable for *in-situ* correction of window transmission in hostile environments. The work described below was a direct industrial application of the technique in the industrial setting of laser heat treatment.

6.0 Traceable temperature measurements for exotic thermal processing methods

Laser surface heat treatment for steel or cast iron parts with high-power diode lasers has been established in industrial mass production during the last 15 years. The purpose of such treatment is to induce a metallurgical change in the surface of the treated imparting hardness of 10 to 100 times greater than possible for the untreated part. Due to the high power density of the laser heat sources and the high processing temperatures, which are often desired to be

close to the melting temperature of the materials, precise temperature measurement and control is essential for the process to yield reproducible results. For the successful heat treatment of special high-alloyed steel grades or gray cast iron surfaces, the process temperature needs to be controlled within a temperature band of only a few degrees Celsius at a temperature of around 1200 °C. Too high a temperature can lead to the part melting and a temperature too low will result in a lower surface hardness and a reduced penetration depths.

One key problem of the temperature measurement by laser and radiation thermometer is the wear and contamination of optical components during their lifetime, e.g. by processing fumes. On-site calibration is needed because the temperature measurement devices are mechanically and electrically integrated into complex machine systems. A second problem is the uncertain emissivity of the surface under treatment. Both these problems were addressed in this research.

6.1 Mobile fixed point for in-situ calibration of radiation thermometers

A mobile induction-heated HTFP device was developed to allow for a calibration in the temperature range 1000–1500 °C and evaluated at industrial set-ups.

Initially different variants of temperature measurement systems, typically used in industrial laser heat treatment, were investigated to define the requirements for the device. The arrangement of system components and processing parameters of the induction-heated fixed-point device were subsequently optimized by a computer simulation with FEM and FDM. Based on the results of that modelling, a prototype of an induction-heated fixed-point device was constructed.

The device consists of a water-cooled and vacuum-sealed housing with ports for connection to a vacuum pump, shielding gas supply, a specially designed lead-through of the induction coils and optical windows. For safety reasons system parameters such as shielding gas flow, water flow and temperature, and residual oxygen content are measured and observed. The fixed point cell is surrounded by graphite felt insulation and held in a ceramic container placed in the induction coil.

Fixed-point cells of Cu, Fe-C, Co-C that could be used with the induction furnace were manufactured at PTB. The fixed-point cells cover the temperature range from 1084.6 °C to 1324 °C. To take account of the different measurement spot sizes of typical industrial radiation thermometers two cell designs with 3 mm and 5 mm diameter cavity diameter were developed.

Different factors influencing the accuracy and reproducibility of the fixed-point plateau temperatures were experimentally investigated, i.e. the position of the fixed-point cell relative to the induction coil, the arrangement of the thermal insulation, the parameters for overheating and undercooling of the cell to initiate the melt and freeze of the metal alloy and variations in the induction frequency. Good results were obtained with repeatability of the fixed point plateau being of order, at worst, of ±0.5 °C. The inductive furnace can be seen in the lower left hand corner of Figure 16. Details of the system can be found in [27].

In the next step the fixed point device was used to evaluate the absolute accuracy of the temperature measurement systems in industrial laser hardening set-ups at Fraunhofer IWS and Alotec Dresden GmbH, Germany. The *in-situ* calibration set-up is given in Fig. 16. Large deviations of up to several 10 K were found in these set-ups, which originate from the large uncertainties of the initial onsite calibration and from continuous wear and contamination of the optical set-ups from process fumes and mechanical damage to the optical surfaces.

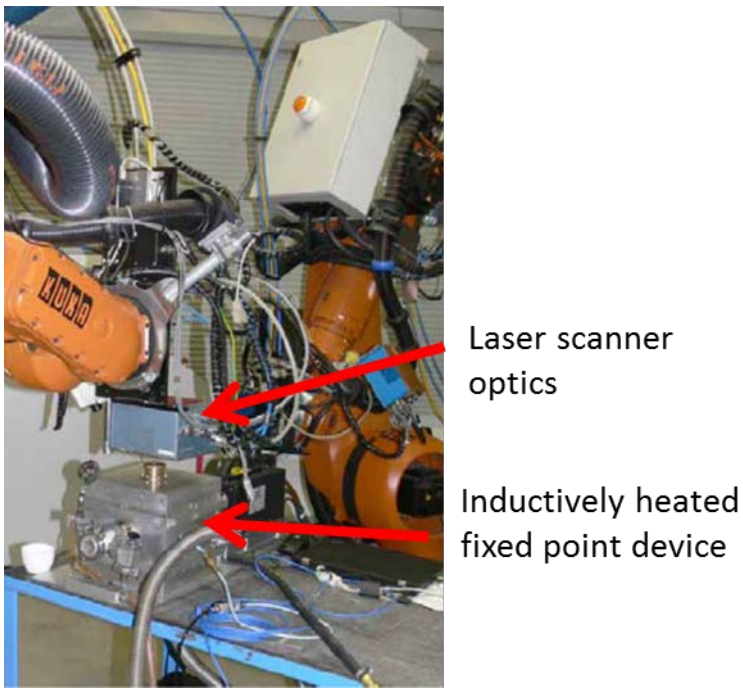

Figure 16: Setup for on-site calibration of laser scanner optics with an integrated thermal imaging system at a machine for industrial laser hardening of steam turbine blades (Fraunhofer IWS Dresden, Germany)

6.2 Emissivity measurements of materials typically undergoing laser hardening

Besides understanding the measurement accuracy of the radiation thermometer, a precise knowledge of the spectral emissivity of the work piece is necessary for a reliable temperature measurement. However direct and accurate emissivity measurement is generally not achievable and hence the values of emissivity can often only be roughly estimated with the help of tables. This significantly adds to the uncertainty of the temperature measurement.

For this reason, the influence of laser hardening and heat treatment on the emissivity of typical steels and cast iron was investigated in the temperature range up to 1300 °C by ZAE Bayern, PTB and SMU. The investigated materials were steels of grade 1.1730, 1.2344, 1.2379 and 1. 4548 and cast iron GGG-70 [28].

For all materials and in the spectral range between 1 and 10 micrometres the spectral emissivity was found to increase with the surface roughness (from polished to a turned to a sandblasted surface in increasing order).

Heat treatment under oxidising conditions results in oxide layer growth on the parts surface. Towards longer wavelength (between 5 and 10 micrometres) the growing oxide layer was observed to change the spectral emissivity drastically, i.e. from around 0.2 to 0.7, whereas for lower wavelengths (<1 micrometre) after an initial step change in emissivity with the build up of the oxide layer from around 0.5 to 0.8 the spectral emissivity was observed to change only slightly. (Figure 17)

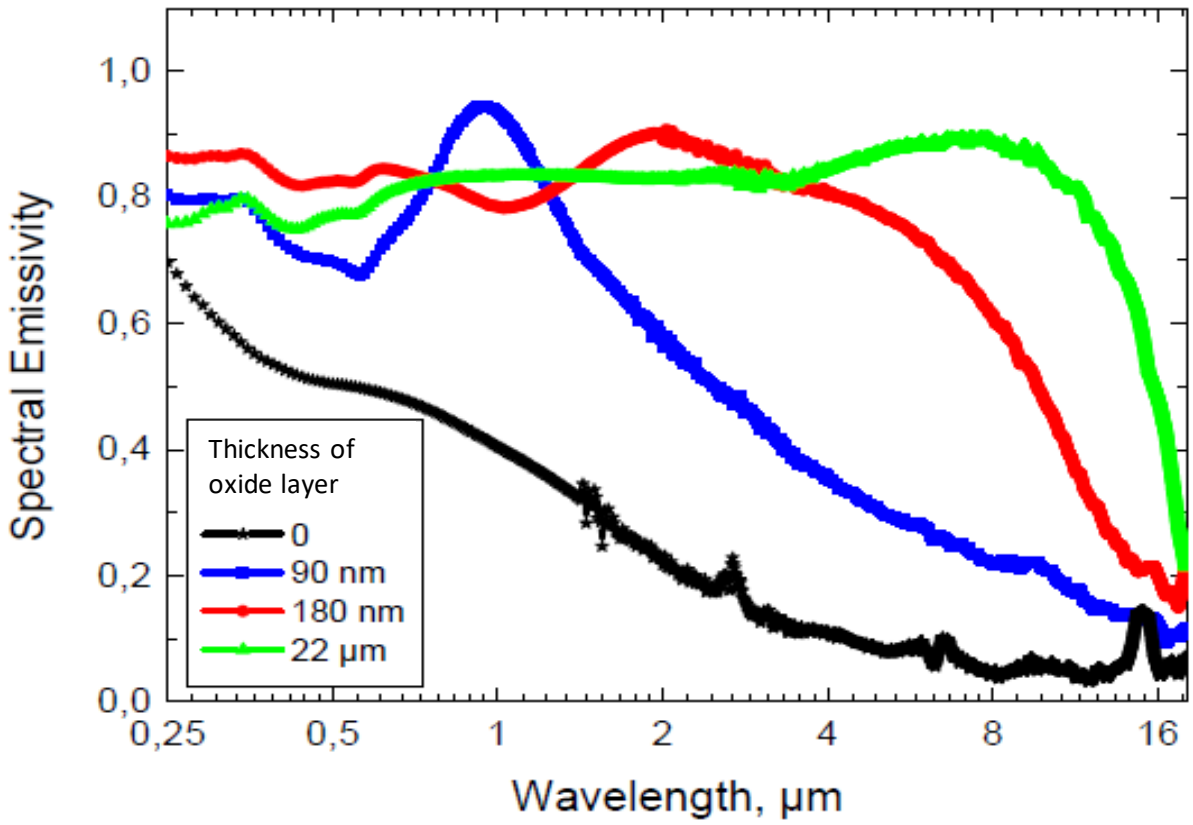

Figure 17: Influence of a growing oxide layer on the spectral emissivity of a steel sample. The layer thickness was determined by cutting the samples after exposing the samples for 20 min to 400 °C (90 nm) and 500 °C (180 nm) and after laser hardening (22 µm)

By combining the emissivity measurements and the *in-situ* calibration of the radiation thermometer it is possible to introduce rigorous traceability into the surface temperature measurement for laser heat treatment, with reliable uncertainty.

7.0 Establishment of reference functions for non standard thermocouples

The purpose of this research was to develop a distributed capability within the EU for the determination of metrological quality low uncertainty reference functions of non-standard high temperature thermocouples. This reference function facility is fully traceable to the

International Temperature Scale of 1990 (ITS-90). Its utility has been demonstrated through application to the characterisation of the Pt-40%Rh / Pt-20%Rh (Land-Jewell) thermocouple. The Land-Jewell thermocouple is useful for continuous use to 1800 °C and occasional use to 1850 °C.

In total, four thermocouples were prepared, designated TC3, TC4, TC5, and TC6, for two phases of reference function determination. Phase 1 comprised TC3 and TC4, both made of wires from the same batch. Phase 2 comprised TC5 and TC6 made from wires of a different batch. The thermocouples were sent between the participants by courier.

Four National Measurement Institutes (NMIs) have participated in this activity. These are CEM (Spain), LNE-CNAM (France), NPL (United Kingdom) and SMU (Slovakia). A range of fixed points, including HTFPs, were employed by all partners; in addition CEM and SMU employed comparison with radiation thermometers. Calibration facilities available, the temperature ranges, and uncertainty on the calibration measurement are summarised in Table 3.

NPL				CEM				SMU				LNE-Cnam			
Type	T / °C	U / μV	U / °C	Type	T / °C	U / μV	U / °C	Type	T / °C	U / μV	U / °C	Type	T / °C	U / μV	U / °C
Sn FP	231.93	1.1	1.7	Cu FP	1084.62	1.7	0.5	Ag FP	961.78	2.1	0.8	Au FP	1064.18	2.3	0.7
Zn FP	419.53	1.2	1.1	Co-C FP	1324	2.7	0.7	Comp	900 - 1200	4.6	1.3	Pd FP	1553.4	6.7	1.5
Al FP	660.32	1.8	0.9	Comp	1200 - 1550	3 - 4.5	0.8 - 1.1					Pt FP	1768.2	9.6	2.1
Ag FP	961.78	3.7	1.3												
Cu FP	1084.62	3.7	1.2												
Co-C FP	1324.29	6.7	1.7												
Pd-C FP	1491.5	8.5	2.0												
Pt FP	1768.2	19.3	4.3												

Table 3: Summary of calibration facilities used by the partners: type of calibration apparatus (FP: fixed point, Comp: comparison with reference thermometer), temperature *T*, and overall uncertainty of the thermocouple calibration U, including thermoelectric inhomogeneity effects (coverage factor $k = 2$).

The calibration measurements performed by each partner are shown in Figure 18, expressed in terms of the difference between the measured emf and the emf given by the reference function in ASTM E1751-09. Figure 18 shows significantly different behaviour of the Phase 1 and Phase 2 thermocouples. This is probably due to the two batches of thermocouple wire having slightly different compositions. Figure 18 shows a discrepancy in the measurements between about 1500 °C and 1750 °C, for both the Phase 1 and Phase 2 thermocouples, indicating an inconsistency between the current measurements and the ASTM reference function.

To determine a draft 'reference function' based on the four thermocouples, all data were combined, and a 5th order polynomial was fitted to the ensemble using the least-squares method, weighted by the uncertainty of the measurements, as shown in Figure 19. The best-fit polynomial has the form

$$E = a_0 + a_1 T + a_2 T^2 + a_3 T^3 + a_4 T^4 + a_5 T^5$$

where *T* is the temperature in units of °C and E is the emf in units of µV. The fitted reference function is shown in Figure 19, together with the combined calibration data. The significantly higher emf at the Pt melting temperature, amounting to an equivalent temperature of between 2 °C and 6 °C (Figure 18), compared with that of the published reference function in ASTM E1751-09 is clear in Figure 18.

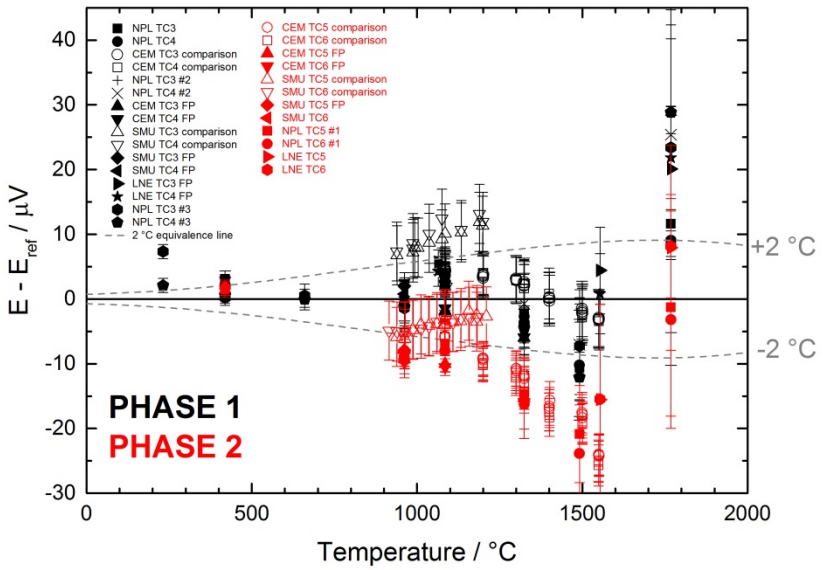

Figure 18: Difference between measured emf and the ASTM reference emf, showing a sharp increase in emf above about 1500 °C.

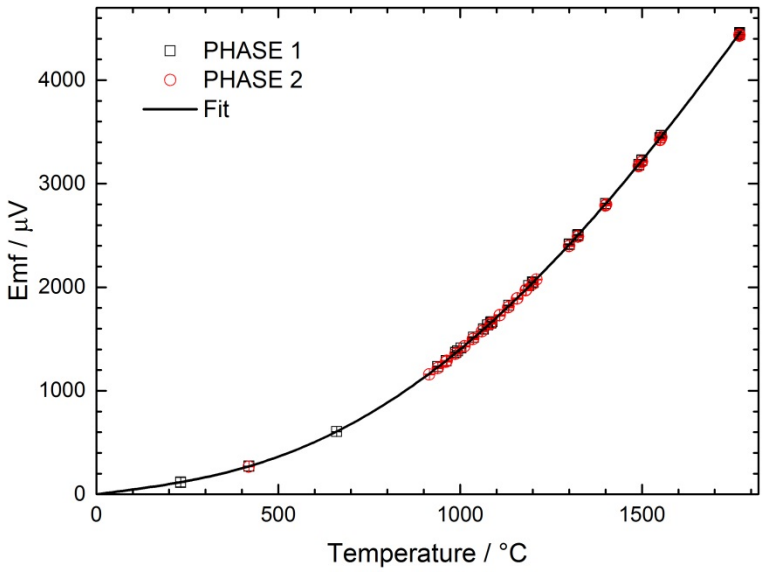

Figure 19: Measured emf as a function of temperature for Phase 1 (TC3 and TC4), black squares, and Phase 2 (TC5 and TC6), red circles. Fitted reference function, black line. Note the good linearity above about 1300 °C.

Some disagreement between these results and the current standard reference function given in ASTM E1751-09 was observed above about 1500 °C. This disagreement is thought to arise from the values of the Pd and Pt melting temperatures that were used in 1965 by Bedford [29] for the generation of the reference function in the *de-facto* standard ASTM E1751-09, which were too low by 1 °C (Pd) and too high by 3 °C (Pt). The Land-Jewell thermocouple is of great utility above about 1500 °C and the current work lays the ground for a revised determination of the reference function for this thermocouple type, and future development of an international standard reference function [30].

Summary

This paper has summarised the main achievements of the EMRP project HiTeMS. Of necessity many details have been omitted because of space constraints – these can be found in the references. However it is clear that significant progress was made towards solving long standing issues regarding the measurement of both contact and non-contact thermometry at high temperatures. This would not have been possible without the pooling of resources and expertise across the EU both within the NMI, industry and research centre community. Some of these findings are being taken forward in the follow EMPRESS project (enhanced process efficiency through improved temperature measurement) [31] part funded by the EMRP successor programme EMPiR[3] (European Metrology Programme for Innovation and Research).

Acknowledgments

GM, JP acknowledge funding from the Engineering and Flow Programme funded by the National Measurement Office. The EMRP is jointly funded by the EMRP participating countries within Euramet and the European Union.

References

[1] Preston-Thomas, H., *Metrologia*, **27**, 3-10, p. 107 *errata* (1990)

[3] More information on EMPIR can be found at http://www.euramet.org/index.php?id=research-empir

[2] Machin, G., Anhalt K., Edler, F., Pearce J., Sadli M., Strnad R., Veulban, E., **HiTeMS: A project to solve high temperature measurement problems in industry**, AIP Conf. Proc. **1552**, 958, doi: 10.1063/1.4821414, (2013)

[3] Machin, G., Anhalt K., Edler, F., Pearce J., Sadli M., Strnad R., Vuelban, E., "**Progress report for EMRP project "High Temperature Metrology for Industrial Applications**", 16th International Congress of Metrology 15001 (2013), EDP Sciences (2013)

[4] Machin, G. & Ibrahim, M., "**Size of Source Effect and temperature uncertainty I: high temperature systems"**, In: *Tempmeko99, The 7th International Symposium on Temperature and Thermal Measurements in Industry and Science,* Delft, The Netherlands, Eds. J. Dubbeldam & M. J. de Groot, Published: IMEKO/NMi-VSL ,p. 681-686 (1999)

[5] Vuelban, E. M., Girard, F., Battuello, M., Nemeček, P., Maniur, M., Pavlásek, P., Paans, T., "**Radiometric techniques for emissivity and temperature measurements for industrial applications**", *submitted to Int. J. Thermophys.*, (2014)

[6] P.B. Coates., *High Temp. High Press.*, **20,** 443 (1988)

[7] Battuello, M., Girard, F., "**Characterisation and laboratory investigation of a ultraviolet multi-wavelength measuring system for high-temperature applications**" *Meas. Sci. Technol.*, (under review 2015)

[8] Bart, M., van der Ham, E. M. W., Saunders, P., *Int. J. Thermophys.*, **28** 2111 (2007)

[9] Vuelban, E. M., *Meas. Sci. Technol.*, **24** 105007 (2013)

[10] *Gold cup results paper by Edgar*

[11] EURAMET guide on lifetime and drift/stability assessment of industrial thermocouples, to be published, 2015

[12] reference wrt homogenity

[13] Failleau G., Arifoviç N., Deuzé T., Diril A., Duris S., Langley M., Pearce J.V., Sadli M., Strnad R.: Investigation of the DRIFT of A batch of base metal thermocouples at high temperature, Symposium on temperature and thermal measurements in industry and science, Tempmeko 2013,14-18. October 2013, Madeira, Portugal, Abstracts book, ISBN: 978-972-8574-15-4, (2013).

[14] Diril

[15] Radek

[16] White, D. R., *et al*, *Metrologia,* **33**, 325 (1996)

[17] Brixy ,H., Hecker, R., Höwener, R., Rittinghaus, K. F, "**Applications of noise thermometry in industry under plant conditions**", *Temperature, its Measurement and Control in Science and Industry,* **5** (Ed. by Schooley) New York, , AIP, 1225-1237 (1982)

[18] Elliot, C.J., Large, M. J., Pearce, J. V., Machin, G., *Int. J. Thermophys.*, **35**, 1202-1214, (2014)

[19] Edler, F., "Miniature fixed points at the melting point of palladium", *Proc. TEMPMEKO 1996* (Ed. P Marcarino, Levrotto & Bella, Torino), 183-188 (1997)

[20] Failleau, G., Elliott, C.J., Deuzé, T., Pearce, J.V., Machin, G., Sadli, M., *Int. J. Thermophys.*, **35**, 1223-1238 (2014)

[21] Mokdad, S., Failleau, G., Deuzé, T., Briaudeau, S., Kozlova O., Sadli, M., "**A self-validation method for high-temperature thermocouples under oxidising atmospheres**", *Int. J. Thermophys., submitted 2015*

[22] Edler, F., Kühne, M., Tegeler, E., *Metrologia*, **41**, 47-55 (2004)

[23] Sadli, M., Bellin-Croyat, T., Bourson, F., Deuzé, T., Diril, A., Failleau, G., Journeau, C., Lowe, D., Mokdad, F., Parga, C., Richard, N., "**High-Temperature Fixed Points for Industrial Applications**" *Submitted to Int. J. Thermophys.*, (2015)

[24] Parga, C., Bourson, F., Sadli, M., Journeau, C., "**Cellules à points fixes de température pour la recherche appliquée**" *In: Proceedings of Congrès de la Société Française de Thermique SFT-2013*, Gérardmer, 28-31 May 2013.

[25] Lowe, D., Bourson, F., Journeau, C., Machin, G., Parga, C., Sadli, M., "**Correction for window transmission in radiation thermometry using high temperature fixed points**", *16th International Congress of Metrology*, 15003 (2013), EDP Sciences 2013

[26] Lowe D., Machin, G., Sadli M., "**Correction of temperature errors due to the unknown effect of window transmission on ratio pyrometers using an in-situ calibration standard**", *submitted to Measurement* (2015)

[27] Seifert, M., Anhalt, K., Baltruschat, C., Bonss, S., and Brenner, B, *J. Sens. Sens. Syst.*, **3**, 47-54, (2014)

[28] Seifert, M., Anhalt, K., Baltruschat, C., Lenhart-Rydzek, M., Brenner, B., Bonss, S., *HTM - journal of heat treatment and materials*, **69** S.182-191, (2014)

[29] Bedford, R.E., *Rev. Sci. Instrum.*, **36**, 1571-1580 (1965)

[30] Pearce, J.V., Hernandez, M.J., Elliott, C.J., Greenen, A., del Campo, D., Pavlasek, P., Nemecek, P., Failleau, G., Deuzé, T., Sadli, M., Machin, G., *Meas. Sci. & Technol.*, **26** doi:10.1088/0957-0233/26/1/015101, (2015)

[31] Pearce, J.V., Edler, F., Elliott, C.J., Machin, G., Rosso, L., Sutton, G., MacKenzie, S., **EMPRESS – A European project to enhance process efficiency through improved temperature measurement,** *submitted to Metrologie 2015, Paris*